A Numerical Study of Short Wave-Long Wave Interaction and Related Surface Cyclone Development

MIKDAT KADIOGLU AND STEPHEN MUDRICK

Department of Atmospheric Science
University of Missouri-Columbia
Columbia, MO 65211

May 1988

Contribution from the Missouri Agricultural Experiment Station Journal Series Number 10587.

ABSTRACT

A nonlinear, 3D, dry, inviscid, quasi-geostrophic channel model is used to study the process of a short wave trough moving through a long wave trough on a mid-latitude beta plane. We wish to gain an understanding of how the modification of the surface cyclone associated with the short wave comes about as it moves through the long wave trough and interacts with it.

A zonally independent, unstable basic state simulating the mid-latitude westerly jet stream has two small amplitude perturbations superimposed upon it. These are a long wave (wave 1) and two short waves (wave 2); their structures are those of the fastest growing normal modes of the basic state, for modes possessing a wavelength equal to the channel length (wave 1) and equal to one half of the channel length (wave 2). The short waves amplify and propagate eastward more rapidly than does the long wave and a short wave trough moves eastward through the long wave trough.

Two runs are discussed, one with both the long wave and the two short waves present initially and the other with only the two short waves. Emphasis is placed on what occurs within vertical columns directly above the surface cyclone centers associated with the short waves.

The major finding is that the surface cyclone associated with the short wave trough moving through the long wave trough deepens more, more rapidly and for a longer time than does the surface cyclone in the short wave only run. This occurs because, as the short wave trough moves eastward of the long wave trough after day 4, the westward slope of the pressure trough with height

above the cyclone center is re-established, whereas for the short wave only surface cyclone the slope has become and remains more vertical by about day 3. This re-establishment allows the differential buoyancy (temperature) advection to become enhanced, up to mid-tropospheric levels, for the two wave run relative to the short wave only run.

1. Introduction

Studies by Bjerknes (1937), Rossby (1939, 1942), Namias (1943), Namias and Clapp (1944), Fultz (1945) and others have demonstrated that the mid-tropospheric westerly wind flow pattern often has distinct sizes of wavelike perturbations associated with it. These disturbances commonly are called long and short waves (hereafter LW and SW, respectively).

The movement of these waves in the upper westerlies and their relationship to the development of surface cyclones were first discussed by Bjerknes in an article published in 1937, according to Neiburger et al. (1982). Subsequently, Rossby studied the dynamics of these waves in detail and derived formulas for their speed (Rossby and Collaborators, 1939).

In general, the shorter the wavelength the greater is the eastward propagation speed of the upper level waves, so we usually find the upper level SWs propagating eastward through the LW pattern. Because these SWs are usually associated with the surface cyclones and anticyclones their behavior is an important part of the forecast problem.

As the SWs move through the LWs, the waves interfere with one another, thus producing a complex pattern. Many of the earlier studies, for want of any better way to proceed, used a linear superposition model of the interaction (see for example, Riehl et al., 1952 p12; Godske et al., 1957, p782). Consider the situation we will be studying: a SW propagates downstream (eastward)

from the LW upstream ridge (LWR) around and through the LW trough (LWT). Fultz (1945), as discussed in Godske et al. (1957), summarizes the process as follows. First of all, the SW will move east-southeastward (when to the west of the LWT) and at the same time the SW trough (SWT) "deepens", i.e. increases its amplitude as it approaches and overtakes the LWT. (Hereafter the time of passage of the SWT through the LWT will be indicated by "SWT→LWT".) Then, it will move east northeastward (when east of the LWT) and it often "weakens" as it moves toward the downstream LWR.

Namias and Clapp (1944) first used Rossby's LW concept in prognosticating the movements of waves on 5-day mean charts (Palmén and Newton, 1969 p152). Then, Fultz (1945) gave some empirical results as "rules of thumb". Later, Cressman (1948) studied the various methods of forecasting the LW and their interactions with smaller waves for short period forecasting. The relationships between the upper-level wave patterns and sea level developments in middle latitudes were investigated and literature on this subject was summarized by Riehl et al. (1952). Interactions between SW and LW are discussed by Petterssen (1956). Yet all these studies seem to be highly qualitative with emphasis on simple empirical forecast rules for the cyclones associated with the SWs.

The purpose of this study is to present some results of a preliminary investigation of the mid-tropospheric wave patterns and their relation with surface cyclones, along with an attempted explanation by using a numerical model.

2. Methodology

a. Description of the model used

A Boussinesq formulation of a quasi-geostrophic model is used in this study. The model used here is restricted to dry, hydrostatic, adiabatic motion. The atmosphere is simulated by an east-west reentrant channel with rigid horizontal and vertical boundaries, located on a mid-latitude beta plane. The artificial effect of the walls is minimized by selecting initial conditions such that nothing happens near the walls. No topography is present.

The flow is assumed to be inviscid, since a basic understanding of the dynamics of atmospheric wave motion can be gotten with the neglect of moisture and radiation effects (e.g., Pedlosky 1987, Charney 1947, Eady 1949). While details of the evolution will certainly be affected by surface friction, the results of Mudrick (1974, 1982) among others, demonstrate that realistic cyclone scale disturbances can be modelled without friction.

The fully three-dimensional, nonlinear, frictionless, quasi-geostrophic (QG) model is described and referenced in sections 3 and 6 of Mudrick (1982).

For the model integrations, a channel length L=5200 km, width $D=6066^{2}/_{3}$ km and depth H=15 km are used. The resolution is fairly coarse, with $\Delta x,\Delta y=216^{2}/_{3}$ km, $\Delta z=1.5$ km; this corresponds to 26x30x10 gridpoints for each variable, with a timestep of 40 minutes. Ten vertical levels are used. The INT filter was used on the potential vorticity field once each timestep (see Mudrick,

1982, section 6).

b. The basic and initial states

The zonally independent basic state used to model the mid--latitude, westerly jet within which the waves and associated surface cyclones develop is similar in structure to the basic state described in Mudrick (1982), see especially Fig. 1 and Table 1. The major differences, as given below, are in some of the parameters.

For the troposphere, a temperature lapse rate of 7.5°C km^{-1} is used, and a stratospheric temperature increase with height of 2.0°C km^{-1}, with a temperature of 246K at 5 km (≈ 540 mb). The squared buoyancy frequencies N^2 used are 5.42×10^{-4} s^{-2} and 0.916×10^{-4} s^{-2} for the stratosphere and troposphere, respectively. The troposphere value is slightly less than the average stability but not unrealistically small; the value was needed in order to satisfy the criteria discussed in the next section. For our case, other parameters describing the basic state characteristics are as follows: $f_0 = 1 \times 10^{-4}$ s^{-1} (corresponding to 43°N), $U_0 = 0$ m s^{-1}, $U_M = 40$ m s^{-1}, $U_T = 30$ m s^{-1}, D_J the jet width = 2000 km, Y_J the location of the jet midline = $3033\frac{1}{3}$ km. Fig. 1 in Mudrick (1982) summarizes the above and shows a jet skewed to the cyclonic side while the jet used here is not skewed.

With the basic state given, a particular channel length was chosen and the most rapidly growing normal mode for that channel length was found by using a procedure similar to that of Brown (1969). The linear QG model used for this purpose is described in

Mudrick (1979). In this study, two such normal mode disturbances were found. One, the "long wave", had a wavelength equal to the channel length itself, 5200 km; the second, the "short wave", had a wavelength equal to half of the channel length, 2600 km, so two short waves would be present in the channel. Both perturbations were superimposed on the basic state. The perturbation amplitudes were chosen to be small, the maximum N-S perturbation wind component being set to 10% of the maximum zonal basic state wind, for both perturbations, so that initially the growth would be linear. This superposition gives the streamfunction, which is the initial pressure field, for the nonlinear QG model.

c. The experiment

The purpose of the integration was to model the SWT→LWT and to study the interaction that occurs with this process. The basic state needed to be chosen such that it was fairly realistic and such that the following criteria were satisfied: 1) the SWs would grow more rapidly than the LW, 2) the SWs would propagate eastward more rapidly than the LW and 3) both LW and SW disturbance amplitudes would be relatively "deep", i.e., they would possess large disturbance amplitudes at jet stream level.

The first criteria allows us to study mainly the evolution of the SWs, compared to the LW. The third criteria hopefully allows deep disturbances to form in conjunction with the SW and favors more vigorous surface as well as upper tropospheric activity.

After several modifications, a basic state was found that

produced satisfactory results. The characteristics of this basic state have been discussed above.

Two runs will be discussed here. The initial state, as described above, with both LW and SWs present, is referred to as the 2-wave run, or 2W. The location of the SWs were initially such that the SWTs were located at the same location as the long wave ridge (LWR) and LWT. The second run had the LW amplitude set to zero so only the SWs were present; this is referred to as the SW run. All runs were carried out to 16 days but we will be interested only in first 8 days or so.

As a check on the behavior of the model, a comparison of the early growth and movement of the SW and LWs was made with the predictions of linear QG theory gotten when the perturbation structures were determined. The overall growth rate and movement of the waves during the first day was considered to be satisfactory, compared to linear QG theory. A Fourier decomposition of the pressure data at an east-west row near the channel center was used to make this comparison.

3. Fourier analysis of trough positions. Labeling of short waves 1 and 2

The time of passage of the SWT into the LWT (SWT→LWT) will be used as a reference time so we can discuss what happens before, during and after this time. For a particular E-W row of pressure data, the phases or positions of the troughs of waves 1 and 2 (the LW and SW, respectively) can be found. Then day to day locations can be noted, so the time of SWT→LWT can be determined. Looking at Fig. 1, which shows in part the pressure at level K=5 for the 2-wave runs, we can see the SWT→LWT process illustrated (2W K=5 Days 3-5).

We will refer to the SWT originally located within the LWT as short wave 1 (SW1) and its trough as SWT1. Thus SWT2 initially lies in the vicinity of the LWR. The surface (K=1) low pressure regions, or cyclones, associated with SWT1 and SWT2 will be referred to as L1 and L2.

Having labeled our disturbances, we will proceed to determine the time of SWT→LWT for this model. Following Table 1 and Fig. 1, (i.e., consider the row of data for j=16, K=5, i varies) we see both SW and LW propagate eastward for the first two days or so, with the short waves moving more rapidly eastward. SWT2, the more eastward SWT initially at the LWR, is seen to move eastward, off the east edge of the domain. It reappears on the west edge due to the cyclic boundary conditions and moves into the region of the LWT. This appears to happen about day 4 (Fig. 1, 2W K=5 Day 4). Table 1 confirms the SWT2→LWT for j=16 is just after day 4 (day 4

is underlined).

The Fourier decomposition procedure was applied for each day, for east-west rows j=13, 16 and 19 and at levels K=3, 5 and 7. Thus 9 east-west rows of data were sampled and the times of SWT2→LWT were averaged to get a more representative value than just using the j=16, K=5 data in Table 1. The average value determined is SWT2→LWT=day 4.17. It will suffice to refer to this time as day 4.

4. Comparison of the 2-wave and short wave only integrations

We will take a look at how the 2W L2 center develops differently than the SW L2 center due to the presence of the LWT through which SWT2 passes. Since the SWs are nearly identical in the SW run (see Fig. 1 SW K=1 and K=5 columns), either of the SW surface cyclone centers can be compared to the 2W L2 center and we have labeled the left center in Fig. 1 SW K=1 Day 3 as "L2".

We will analyze various quantities in a vertical column extending over 2W L2 and compare changes with time to corresponding quantities for a column over the SW low center corresponding to L2. We will emphasize processes related to the enhanced deepening of 2W L2 compared to the SW cyclone and to the behavior of the vorticity in the columns over the low centers.

The following nondimensional equations were derived from the QG model basic equations (see Mudrick, 1974, section 2) and will form the basis for our analysis:

tendency equation ($\chi = \partial p'/\partial t$)

$$(\nabla_H^2 + \frac{1}{N^2}\frac{\partial^2}{\partial z^2})\chi = -\underset{\sim}{v}_G\cdot\nabla_H(\nabla_H^2 p' + f) + \frac{1}{N^2}\frac{\partial}{\partial z}(-\underset{\sim}{v}_G\cdot\nabla_H b),$$

vorticity equation

$$\frac{\partial}{\partial t}\nabla_H^2 p' = -\underset{\sim}{v}_G\cdot\nabla_H(\nabla_H^2 p' + f) + \frac{\partial w}{\partial z},$$

vertical motion (omega) equation

$$(\nabla_H^2 + \frac{1}{N^2}\frac{\partial^2}{\partial z^2})w = -\frac{1}{N^2}\frac{\partial}{\partial z}[-\underset{\sim}{v}_G\cdot\nabla_H(\nabla_H^2 p' + f)] + \frac{1}{N^2}\nabla_H^2(-\underset{\sim}{v}_G\cdot\nabla_H b),$$

and thermodynamic equation

$$\frac{\partial}{\partial t}\left(\frac{\partial p'}{\partial z}\right) = -\underset{\sim}{v}_G\cdot\nabla_H\left(\frac{\partial p'}{\partial z}\right) - N^2 w, \text{ where } \underset{\sim}{v}_G = \left(-\frac{\partial p'}{\partial y}, \frac{\partial p'}{\partial x}\right).$$

For qualitative purposes the above equations can be considered as follows, respectively:

$$\chi \approx - \text{VORT ADV} - D(\text{B ADV}) \quad (1)$$

$$\partial/\partial t \ \text{VORT} = \text{VORT ADV} + \partial w/\partial z \quad (2)$$

$$w \approx D(\text{VORT ADV}) + \text{B ADV} \quad (3)$$

$$\partial b/\partial t = \text{B ADV} - N^2 w \quad (4)$$

These equations are discussed in Mudrick (1974) and in Holton (1979, Ch.6), for the usual constant pressure coordinate system.

We will use (1) through (4) in a qualitative manner, looking at the terms on the right hand sides to estimate the sign of the left hand sides. These will be compared to the day by day changes of various quantities over the low center. Thus, what follows is only a " plausibility argument"; a more complete analysis of the data is planned for future work. Since Fig. 1 shows the SW and 2W pressure patterns for K=1 and K=5, for days 3 to 5, the SW and 2W runs can be compared to see the slope of the pressure trough with height, as discussed below.

Before we consider separately the evolution of the SW and 2W L2 centers, let us look at their central pressure evolution versus time, as shown in Fig. 2. Comparing the QG SW L and QG 2W L2 curves, we see similar development until day 3 or so, whereupon the SW deepening rate decreases and the SW low reaches its lowest pressure at day 5 or so. The 2W center also has its deepening rate reduced (but not as much as the SW center) until day 4, about the time of SWT→LWT. After that time the 2W center expands and increases its deepening rate; the center reaches its lowest pressure

a little after day 6. The passage of the SWT through the LWT seems to reinvigorate the 2W low center.

Fig. 2 also contains results from primitive equation (PE) model integrations designed to be nearly identical to the 2W and SW QG runs. The PE model is designed to run as a comparison to the QG model (Mudrick, 1982). The QG results are seen to be similar to the more realistic (and more complicated) PE runs. For the PE 2W run, SWT→LWT occurred about day 5. The PE runs will not be discussed further in this paper.

We will examine first the evolution of the SW cyclone center, without the complicating effect of the long wave. We will then contrast the evolution of the 2W center.

a. Evolution of the SW Low Center.

We will only briefly summarize the growth stage of the SW center, which lasts until about day 2. Conditions at day 2 typify the situation. During this stage the pressure falls over the center due to VORT ADV >0 and D(B ADV) >0 and the relative vorticity increases over the center due to the positive vorticity advection and low level convergence. We see this as follows. Fig. 3A for days 0-2 schematically shows the situation for levels K=3 to 5; V marks the relative vorticity maximum at K=3 and 5 while L marks the cyclone center at K=1. With the pressure trough sloping westward from L with height and with the P and b isolines at levels K=3 and 5 as sketched, we see VORT ADV >0 and B ADV >0 over L. With the wind speed increasing with height below the tropopause (≈K=7)

we expect D(VORT ADV) >0 and D(B ADV) >0 below this level. Fig. 6 presents data for days 2-6 for the vertical column above the L2 center for both the SW and 2W runs; the day 2 SW data show the above to be true. Fig. 6 also shows the low level convergence for day 2 for the SW case, it is seen to be >0 up to K=4. Fig. 4 shows the pressure change above the L2 center for days 0-8 and for levels K=1, 3, 5 and 7, while Fig. 5 shows the relative vorticity.

By day 3 changes have come about at the SW low center. As indicated by Fig. 3B, the pressure trough at levels up to K=5 now lies over the surface low L, thus, the pressure trough is much more vertical than on day 2. The buoyancy still decreases to the west as well as to the north. The relative vorticity maximum at level K=3 or 5 is now to the east of the trough, as shown at V. Why has the upper level pressure trough caught up with the surface low? As p deepens and the relative vorticity $\nabla^2_H p$ increases over the low center the p trough becomes more vertical. We have seen that the advection of the absolute vorticity, or VORT ADV, increases with height over the low center L. Also the differential buoyancy advection, or D(B ADV), >0 so the pressure falls should be stronger with height, i.e., $\partial p/\partial t$ becomes more negative with height, according to (1). This is true as seen by calculating p(day 3)-p(day 0) for the various levels in Fig. 4. This should work to bring the upper trough more over the low center with time.

Consistent with the vorticity maximum at levels K=3 and 5 being east of the low center, we find VORT ADV < 0 for day 3 in Fig. 6A, becoming more negative with height, up to level K=7, the

jet core level, above which we are not interested. From the SW portion of Fig. 6B we now find cold advection, i.e. B ADV, < 0, over the center, as can be deduced in Fig. 3B. This becomes less negative with height so D(B ADV) > 0. With respect to (1), VORT ADV and D(B ADV) are of opposite signs. Fig. 4 shows a decrease in the rate of deepening of p at K=1, but p is still decreasing.

The results for (2) are more consistent. Fig. 6C shows convergence $\partial w/\partial z < 0$ up to level 4, which, along with VORT ADV < 0 implies $(\partial/\partial t)$VORT < 0. The $\partial w/\partial z < 0$ is consistent with results from (3); since D(VORT ADV) < 0 and B ADV < 0 we expect $w<0$ as is seen in Fig. 6D. We see from Fig. 5 that VORT has reached a maximum at day 3 for K=1.

Beyond day 3 $\partial w/\partial z$ remains small compared to earlier values, and VORT ADV is also fairly small compared to the values of day 0 to 2. Thus in (2) *both terms* are small. From Fig. 5 we see that VORT does not change much after day 3 for K=1, 3 and 5. With respect to (1) beyond day 3, we see from Fig. 4 that p continues to decrease for levels K=1, 3, 5 and 7 to day 5, but by day 4 the deepening has greatly slowed. After day 4, as mentioned above, VORT ADV is fairly small, while at day 4 D(B ADV) varies over K. So $\partial p/\partial t$ would be expected to be small but the expected sign is unclear for day 4. For day 5 D(B ADV) < 0 suggests $\partial p/\partial t > 0$; we see after this time the cyclone center fills.

In summary, the evolution of the SW low center can be stated as follows. Initially the westward slope of the pressure trough with height (Fig. 3A) gives relatively large values for vorticity

advection over the low center. The b values decrease to the west as well as to the north; this orientation gives positive buoyancy advection over the low center. Both increase with height. This is associated with falling central pressure and increasing vorticity.

From about day 3 onward, the pressure trough is nearly vertical over the low center. The effect is to reduce the strength of the advections. The development slows, in general, as the advections become smaller.

b. Evolution of the 2W Low Center

The evolution of the 2W L2 cyclone, as it moves through the LWT, will now be discussed. Its behavior is similar to the SW cyclone through day 2, during which time the effect of the LW presumably is small. This can be seen from Figs. 3A, 4, 5 and 6. In what follows we will concentrate on the period from day 4 on. We will also use L2 to refer to the 2W low center of interest while L will refer to the SW low center.

We will organize this section around two questions: 1) Why does the L2 center in the 2W run continue to deepen from day 4 to 6, whereas the L center in the SW run stops deepening after day 5 (Figs. 2 and 4)? 2) Why does the vorticity over the L2 center decrease after day 4 when there is no corresponding decrease over L in the SW case (Fig. 5)? Both of these differences between the 2W L2 cyclone center and the SW L center appear during or after the time of SWT2→LWT.

Looking at Fig. 6A, we note a major difference between the

2W and SW cases: for days 4 to 6 the VORT ADV is more negative for 2W, throughout the troposphere. The negative VORT ADV is significantly stronger for 2W, for days 4 and 5. This enhanced negative VORT ADV in 2W should answer question 2), using (2). Note $\partial w/\partial z$ from Fig. 6D is positive but fairly small, for days 5 to 6, compared to $\partial w/\partial z$ values for day 2, so it probably has a small effect in (2).

Using (1), the increased negative VORT ADV over L2 should mean, in the absence of D(B ADV), that $\partial p/\partial t$ should be more positive over the L2 cyclone center, compared to the SW L center, for these levels and times. The reverse is true, as seen in Fig. 4. So we must have D(B ADV) for these times tending to be more positive for L2 than for the SW L; this could counteract the vorticity advection effect and allow $\partial p/\partial t$ to be more negative for L2 than for L. For levels K=3 and 5 this is seen to be true for days 4 to 6, from Fig. 6B. We thus can argue that the 2W versus SW B ADV values in Fig. 6B can be consistent with $\partial p/\partial t$ being more negative for L2 than for L, for days 4 to 6.

The greater positive values of D(B ADV) are related to the greater magnitudes of B ADV seen over the L2 center, compared to the L center (again see Fig. 6B). This comes about because the LWT distorts the more simple symmetry of the SWT which is vertically over the L center in the SW case.

First consider the situation at day 4. Fig. 3B can be used for the 2W L2 case with L2 replacing L. We note L2 is further south from the center of the upper low, for the L2 cyclone, than for

the SW cyclone, because of the presence of the LWT, with its pressure minimum superimposed. This also makes the SWT associated with L2 a little sharper than the SWT associated with the L cyclone. So B ADV over L2 can be of greater magnitude, even though both are negative. This allows the D(B ADV) the possibility of being greater over L2 than over L.

At this time, day 4, the vorticity patterns for L2 and L are such that at K=5 and to a lesser extent at K=3 the vorticity maximum is slightly to the east of the surface lows and therefore there is negative vorticity advection over the low centers (Fig. 3B). We will not pursue the question as to why the vorticity maximum is ahead of the surface lows, except to note that since it occurs in both cases it apparently is not related to the presence of the LWT. From data not presented it can be seen that the vorticity pattern over the L2 center is more elongated NE-SW and has a greater gradient than does the pattern over the L center. While the maximum value of vorticity is <u>not</u> appreciably greater over the L2 center, the enhanced gradient due to the distortion associated with the presence of the LWT apparently allows the negative VORT ADV over the L2 center to be stronger than that over the L center.

So at day 4, in the 2W run, the SWT2 being located in the LWT causes distortions in what would otherwise be the SW pattern. The distortions, basically an elongation and narrowing of the troughs, cause the B ADV and VORT ADV to be of greater negative values over the L2 center than in the SW run. The enhanced negative VORT ADV over the L2 center is counteracted by the apparently increased

D(B ADV) values since p continues to deepen in L2, as discussed above.

After day 5 the disturbance in the SW run has become more or less vertical and the advections have decreased in magnitude, compared to day 3 and earlier. From day 5 onward, the L pressure center fills slowly. (Fig. 4). In the 2W situation, however, the pressure over L2 continues to decrease to day 6, as mentioned above. An interesting occurrence is noted. From days 5 to 6, the L2 center is again ahead of, i.e., east of the upper trough at levels K=3 and 5, as it was at days 2 and 3. The situation is again similar to Fig. 3A, with the b isolines oriented over the low center as shown there. The only difference is that the vorticity maximum at K=5 is nearly over the L2 center, <u>not</u> as shown in Fig. 3A. So again B ADV > 0 from days 5 to 6. At day 5 D(B ADV) > 0 for levels K=3 to 7 (Fig. 6B). Meanwhile VORT ADV < 0 at days 5 and 6 but its magnitude decreases from days 4 to 6, as the vorticity center is more over the L2 center again, as in the SW case (Fig. 6A). With the negative VORT ADV magnitude decreasing at day 5, the D (B ADV) > 0 apparently allows p to continue to decrease at day 5 by (1). By day 6 the D (B ADV) becomes less organized in the vertical, consistent with p reaching a minimum and no longer decreasing. Beyond this time the central pressure increases as L2 fills.

It is thus the location of the L2 center east of the upper trough at days 5 and 6, and the related buoyancy advection, that apparently allows the central pressure to continue to fall over

L2. We must investigate how the L2 center becomes east of the upper trough for days 5 and 6, when it was under the trough at day 4. This must be related to the presence of the LWT.

The answer is that the LWT is retrogressing, or moving westward, in the vicinity of the L2 cyclone center, even as the SWT associated with the cyclone wave moves eastward. This causes the observed upper level pressure trough, a combination of the SWT and LWTs, to move westward relative to the eastward moving L2 center at K=1. So the slope redevelops to the west with height from L2.

Evidence to support this is seen in Table 1, which shows the Fourier decomposition for j=16, K=5; the LWT is seen to be retrogressing from day 3 to day 6. Looking at the decomposition data for j=16 and 19 and for levels K=3, 5 and 7 supports this argument. (These data are not presented here.) The average movement of the LWT is 3 grid points westward from days 4 to 5, thereafter it remains fairly stationary to day 7.

The major factor of importance probably is that after day 4 the LWT is to the west of the SWT2, rather than whether the LWT actually retrogresses. The LWT being to the west of the SWT2 works to retard the movement of the upper level pressure trough, relative to the surface center, redeveloping the westward slope of the pressure trough with height. Question 2) is answered.

In summary, we find that the behavior of the 2W L2 cyclone, as it passes through and to the east of the LWT, is still similar in many ways to the SW cyclone behavior. The differences, due to

the presence of the LWT, are significant and are consistent with the behavior of the L2 cyclone as it moves out of the LWT. The L2 cyclone deepens for a longer time and reaches a lower central pressure than does the L cyclone, mainly because the pressure trough slopes westward with height after L2 leaves the LWT to the west. At this time in the life of the L cyclone in the SW run, the pressure trough is vertical. The westward slope above L2 allows the arrangement of the buoyancy advection to be present that is associated with further deepening. The westward slope comes about after SWT2→LWT occurs; this is related to the movement of the SWT2 to the east of the LWT.

5. Summary and conclusions

We have used a numerical model to simulate the process of a short wave passing through a long wave trough (LWT), a situation often seen in mid-latitude atmospheric flow patterns. Two QG model integrations were compared, one with (2W) and one without (SW) the long wave. Emphasis was placed on what happened within the columns directly above the low pressure centers as they evolved. The differences were argued to be related to the action of the LWT on the evolution of the low pressure center within the 2W run. A plausibility argument was carried out by the use of quasi-geostrophic theory.

As the short wave trough (SWT2) moves eastward out of the LWT, the surface cyclone L2 associated with SWT2 undergoes continued deepening, whereas by this time it would have been filling had the LWT not been present (Figs. 2 and 4).

Related to the enhanced deepening is the westward slope of the pressure trough with height that is re-established as the SWT2 moves east of the LWT. Before this time it had become vertical, as had the SWT when no LWT was present. Without the LWT interaction the SWT maintains the vertical orientation of the pressure trough and the cyclone fills slowly instead of continuing to deepen as it does in the 2W case.

This re-establishment of the westward slope with height after the SWT2 passes through the LWT seems to be a significant development resulting from the LWT interaction.

Within the 2W run it appears that enhanced buoyancy advection, increasing in magnitude with height at mid-tropospheric levels, may be associated with enhanced deepening of the cyclone following passage through the LWT.

The evolution of the 2W low center is quite similar to that of the SW low center, showing that the influence of the LWT on the 2W L2 evolution is of secondary importance. The LWT is thus seen to be "weak" in this study. Had a more pronounced LWT been present these results could be quite different.

Acknowledgments. Part of this work was supported by NASA Grant NAG-5-381 and part by the University of Missouri-Columbia Agricultural Experiment Station Grants MO-315 and MO-316. The major computer work described herein was completed by Dr. Mudrick while he was on sabbatical leave at the Department of Atmospheric Science, State University of New York at Albany. The authors are grateful to the Department Chairman at SUNYA, Dr. Richard Orville, and others at both UMC and SUNYA for their technical assistance and invaluable help. This paper was part of a master thesis by Mikdat Kadioglu, who gratefully acknowledges the support of the Turkish Government.

REFERENCES

Bjerknes, J., 1937: Theorie der aussertropischen zyklonenbildung. Meteor. Z., 54, p463.

Brown, John A., 1969: A numerical investigation of hydrodynamic instability and energy conversions in the quasi-geostrophic atmosphere: Part I. J. Atmos. Sci., 26, 352-365.

Charney, Jule G., 1947: The dynamics of long waves in a baroclinic westerly current. J. Meteor., 4, 135-163.

Cressman, G. P., 1948: On the forecasting of long waves in the upper westerlies. J. Meteor. 5, 44-57.

Eady, E. T., 1949: Long waves and cyclone waves. Tellus, 1, 33-52.

Fultz, D., 1945: Upper-air trajectories and weather forecasting. Dep. Meteor. Univ. Chicago. Misc. Rep. no. 19, 121pp.

Godske, C. L., T. Bergeron, J. Bjerknes, and R.C. Bundgaard, 1957: Dynamic Meteorology and Weather Forecasting, American Meteorological Society and Carnegie Institute, 800pp.

Holton, J. R., 1979: An Introduction to Dynamic Meteorology. 2nd Ed., Academic Press, 391pp.

Neiburger, M., J. G. Edinger, and W. D. Bonner, 1982: Understanding Our Atmospheric Environment, 2nd ed. W. H. Freeman and Company, San Francisco, 265pp.

Mudrick, S. E., 1974: A numerical study of frontogenesis. J. Atmos. Sci. 31, 869-892.

_____ , 1979: On the instability of asymmetric jets. J. Atmos. Sci. 36, 1217-1225.

_____ , 1982: A study of the adequacy of quasi- qeostrophic dynamics for modeling the effect of cyclone waves on the larger scale flow. J. Atmos. Sci. 39, 2414-2430.

Namias, J., 1943: Methods of extended forecasting as practiced by the Five-Day Forecasting Section. Washington, U.S. Department of Commerce, Weather Bureau, 64pp.

_____ , and Clapp, P. F., 1944: Studies of the motion and development of long waves in the westerlies. J. Meteor. 1, 57-77.

Palmén, E. and Newton, C. W., 1969: Atmospheric Circulation Systems: Their Structure and Physical Interpretation. Academic Press, New York, 603pp.

Pedlosky, J., 1987: Geophysical Fluid Dynamics, 2nd Ed. Springer-Verlag, New York, 710pp.

Petterssen, S., 1956: Weather Analysis and Forecasting. 2nd Ed. Vol. 1, Chapters 8-10. McGraw-Hill, New York.

Riehl, H., J. Badner, N. E. La Seur, J. E. Hovde, L. L. Means, W. C. Palmer, M. J. Schroder, L. W. Snellman, and Staff, Chicago Forecast Center, 1952: Forecasting in Middle Latitudes. Meterological Monographs 1, no. 5, 80pp.

Rossby, C.-G., 1942: Kinematic and hydrostatic properties of certain long waves in the westerlies. Dep. Meteor. Univ. Chicago. Misc. Rep., no. 5, 37pp.

_____, and Collaborators, 1939: Relation between variations in the intensity of the zonal circulation of the atmosphere and the displacement of the semipermanent centers of action. J. Mar. Res., 2. 38-55.

TABLE 1. East-west location, given value of i index, of long wave trough (LWT), short wave trough 1 (SWT1) and short wave trough 2 (SWT2) for the pressure at level K=5, north-south location j=16. Channel is cyclic so values of i in parenthesis correspond to values of i-24. Positions are determined by a Fourier decomposition. (Underlined numbers represent days closest to passage of the SWT through the LWT.)

DAY	LWT	SWT1	SWT2	DAY	LWT	SWT1	SWT2
0	8.8	8.5	20.5	6	9.5	4.2	16.2
1	10.1	12.0	24.0	7	10.0	8.0	20.0
2	11.0	15.5	3.5	8	9.4	<u>11.0</u>	23.0
3	11.1	18.9	6.9	9	8.8	13.3	25.3
4	10.2	22.0	<u>10.0</u>				(27.2)
				10	7.9	15.2	3.2
		(25.2)					
5	9.8	1.2	13.2				

LIST OF CAPTIONS

FIG. 1 Nondimensional pressure for 2-Wave (2W) and for short wave (SW) runs, for days 3-5 and for levels K=1 and 5.

FIG. 2 Central nondimensional pressure of the 2W and SW cyclones for K=1, PE and QG models.

FIG. 3 Schematic of pressure _____ and buoyancy (temperature) ---- isolines at K=3 and K=5 in vicinity of surface low; pressure trough —·—·—. V marks location of vorticity maximum at K=3 or K=5. L or L2 marks location of K=1 cyclone center. P_{MIN} marks location of pressure minimum at K=3 or K=5.

(A) SW, 2W cases for days 0-2.

(B) SW case for days 3-4 (with L2 removed), also 2W case for day 4 (with L removed).

FIG. 4 Nondimensional pressure over cyclone center versus time, levels K=1, 3, 5 and 7. 2W versus SW.

FIG. 5 Nondimensional relative vorticity $\nabla_H^2 p'$ over cyclone center versus time, levels K=1, 3 and 5. 2W versus SW.

FIG. 6 Quantities over L2 center, 2W (solid lines) versus SW (dashed lines), nondimensional. (A) absolute vorticity, (B) buoyancy, (C) convergence $\partial w/\partial z$ and (D) vertical motion w. Days 2-6 (numbers next to the lines).

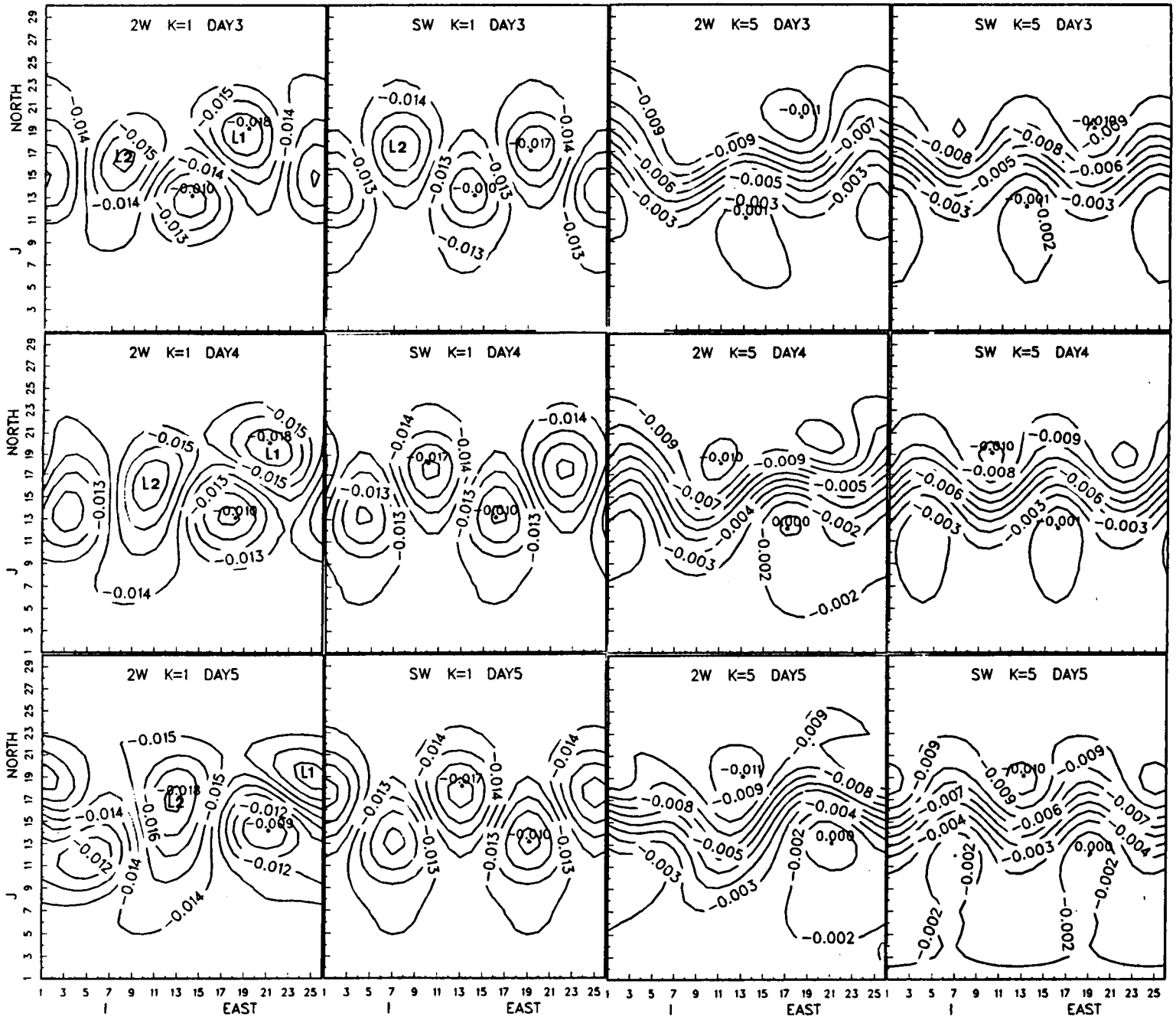
2W K=1 DAY3
SW K=1 DAY3
2W K=5 DAY3
SW K=5 DAY3
2W K=1 DAY4
SW K=1 DAY4
2W K=5 DAY4
SW K=5 DAY4
2W K=1 DAY5
SW K=1 DAY5
2W K=5 DAY5
SW K=5 DAY5
NORTH
J
I
EAST
L1
L2

Fig. 1

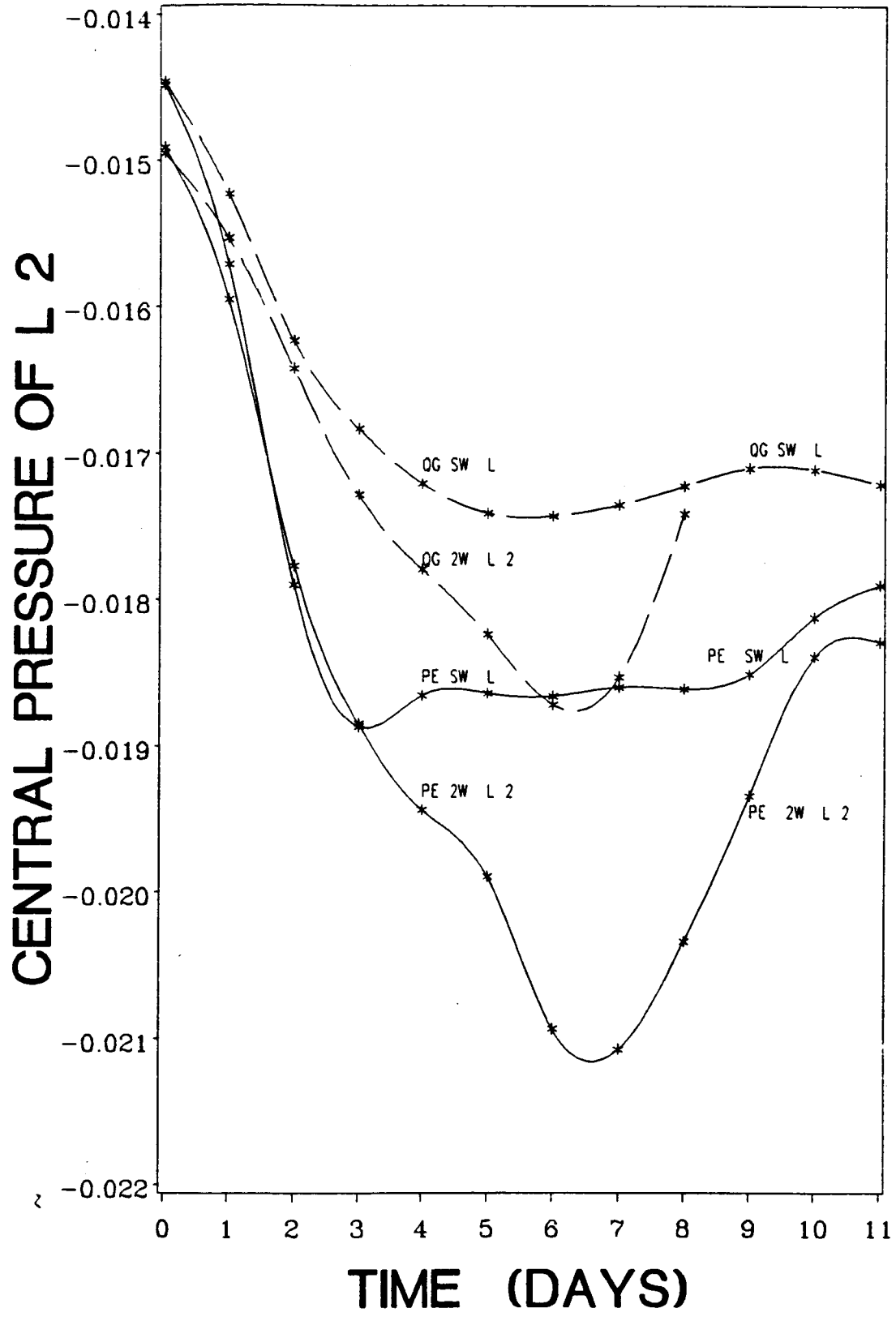
CENTRAL PRESSURE OF L 2
-0.014
-0.015
-0.016
-0.017
-0.018
-0.019
-0.020
-0.021
-0.022
0
1
2
3
4
5
6
7
8
9
10
11
TIME (DAYS)
OG SW L
OG 2W L 2
PE SW L
PE 2W L 2
OG SW L
PE SW L
PE 2W L 2

Fig. 2

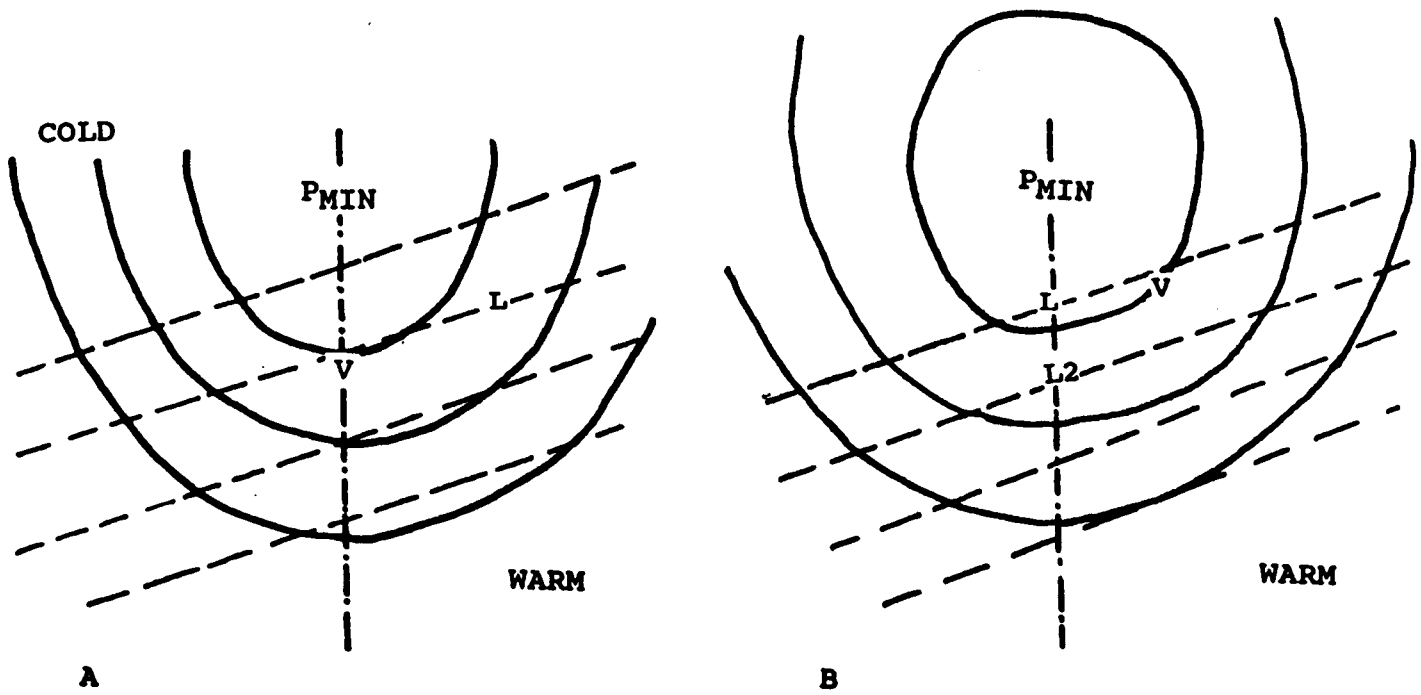

Fig. 3

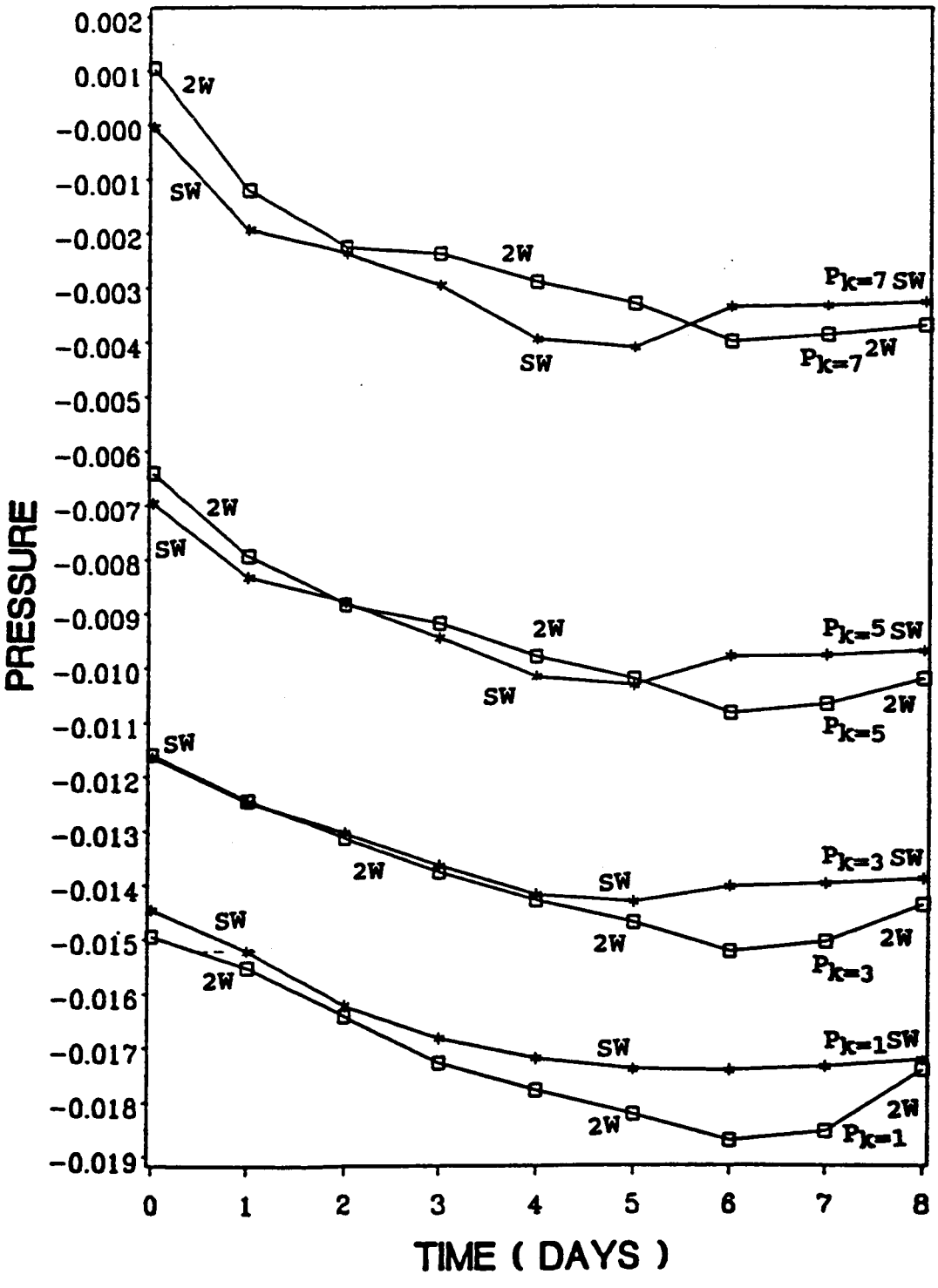
0.002
0.001
-0.000
-0.001
-0.002
-0.003
-0.004
-0.005
-0.006
-0.007
-0.008
-0.009
-0.010
-0.011
-0.012
-0.013
-0.014
-0.015
-0.016
-0.017
-0.018
-0.019
PRESSURE
0
1
2
3
4
5
6
7
8
TIME (DAYS)
2W
SW
2W
SW
Pk=7 SW
Pk=7 2W
2W
SW
2W
SW
Pk=5 SW
2W
Pk=5
SW
2W
SW
Pk=3 SW
2W
SW
2W
Pk=3
SW
2W
SW
Pk=1SW
2W
2W
Pk=1

Fig. 4

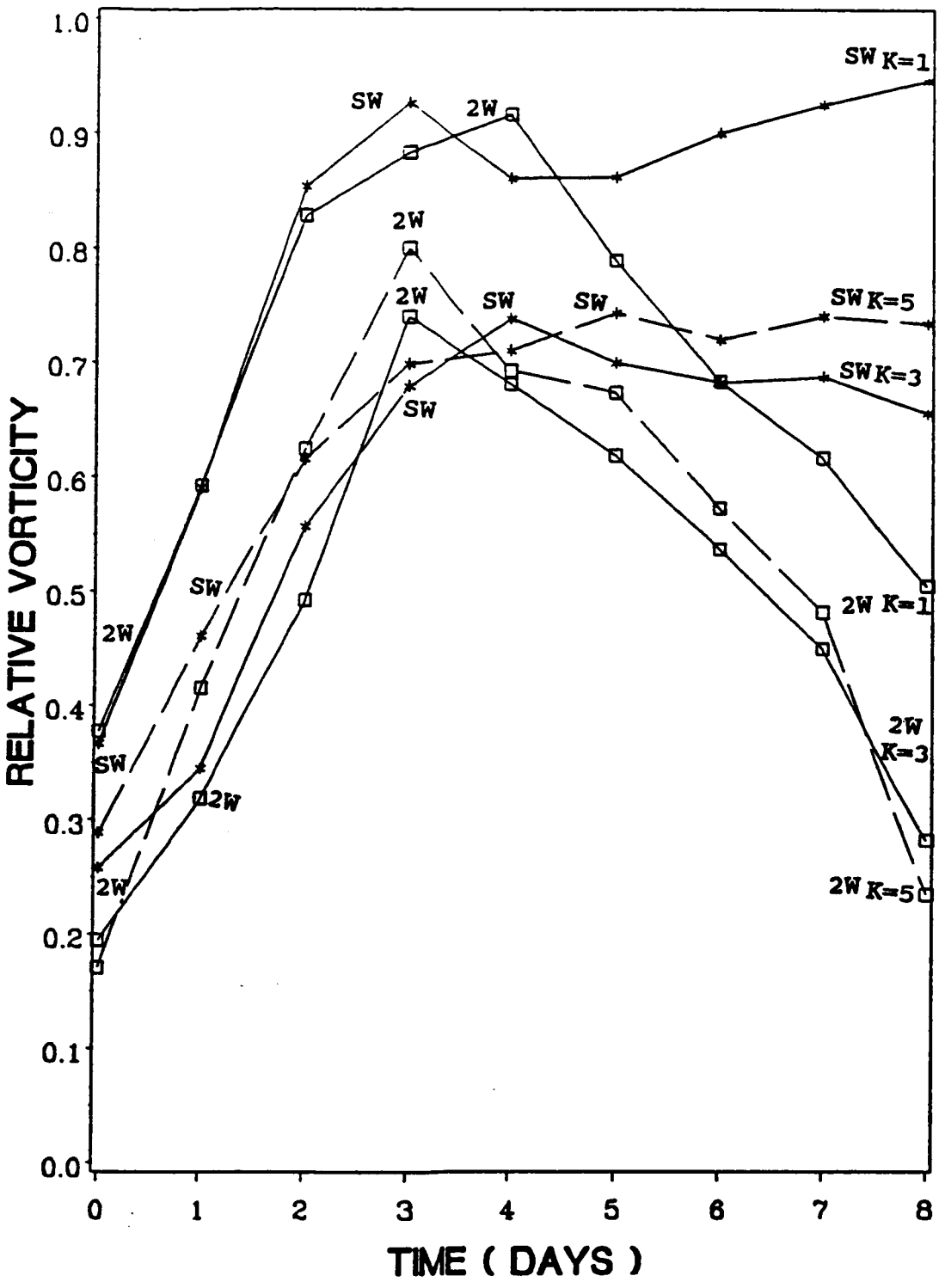
RELATIVE VORTICITY
TIME (DAYS)
1.0
0.9
0.8
0.7
0.6
0.5
0.4
0.3
0.2
0.1
0.0
0
1
2
3
4
5
6
7
8
SW K=1
SW K=5
SW K=3
2W K=1
2W K=3
2W K=5
SW
2W

Fig. 5

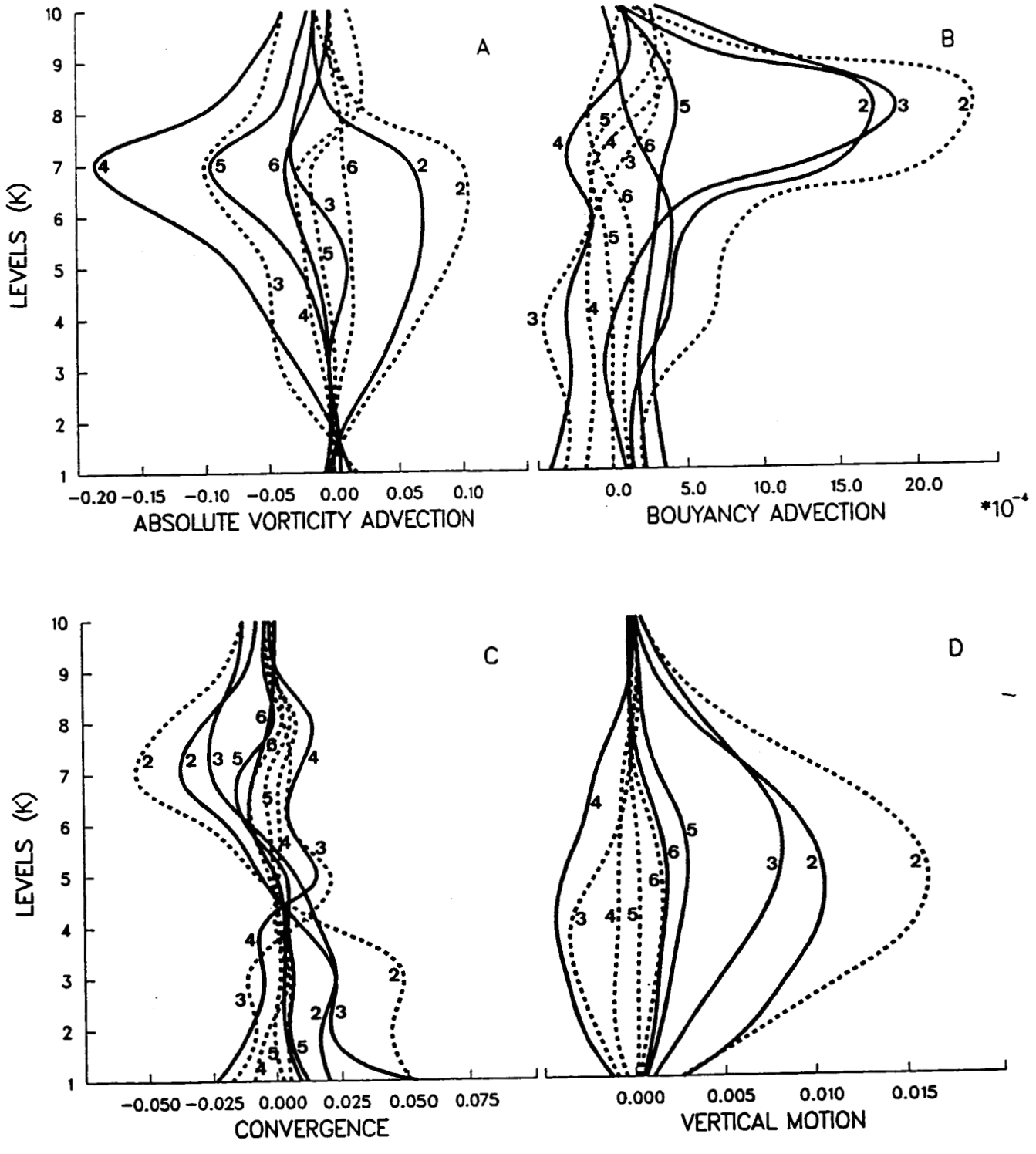
A
B
C
D
LEVELS (K)
ABSOLUTE VORTICITY ADVECTION
BOUYANCY ADVECTION
*10⁻⁴
CONVERGENCE
VERTICAL MOTION
-0.20 -0.15 -0.10 -0.05 0.00 0.05 0.10
0.0 5.0 10.0 15.0 20.0
-0.050 -0.025 0.000 0.025 0.050 0.075
0.000 0.005 0.010 0.015

Fig. 6